

# Tiling algorithm with line-based transform for rapid ship detection and wake feature extraction in ALOS-2 SAR sensor data

Deepika Selvaraj<sup>1</sup>, Elangovan Krishnamurthy<sup>2</sup>, Don Sasikumar<sup>3</sup>,  
Lekshmi Sivankutty<sup>4</sup>, Ganesan Kaliyaperumal<sup>1\*</sup>

<sup>1</sup> Vellore Institute of Technology, Vellore, Tamil Nadu, India

<sup>2</sup> Sri Annai Polytechnic College, Vellore, Tamil Nadu, India

<sup>3</sup> Department of computer science and engineering, Amrita Vishwa Vidyapeetham, Amritapuri, Kerala, India

<sup>4</sup> Naval Physical & Oceanographic Laboratory, Defence Research and Development Organisation, Kerala, India

## ABSTRACT

The satellite PALSAR-2/ALOS-2 image plays a vital role in marine environment protection, weather analysis, and other geophysical processes. Satellite image processing is requiring more time to extract the different features in the ocean region. In this article, the proposed tile-based iteration technique along with line transform for high-speed ship detection and wakes feature extraction in the PALSAR-2/ALOS-2 image. The standard noise removal/despeckling techniques are applied to the SAR data to get accurate information about the ship for detection and wake features for velocity estimation. The despeckling performance is evaluated by the metrics called Edge Preservation Index (EPI) and Structure Similarity Index (SSIM) metric. Furthermore, the proposed tiling and region-based morphological operation are applied to the despeckled SAR image for ship detection and the results are compared with an exciting method. Line-based Radon and Hough transform has estimated the angle and wavelength of the ship wake lines which are present behind the ship. The article is focused on rapid ship detection and feature extraction which consumes only 160 seconds to process the tile-based combination of image size  $1978 \times 2536$ , 7 times faster than without tiling algorithm. To demonstrate the proposed work, the test environment is created using MATLAB and the result proves that 1.0x to 1.5x faster than the standard existing method.

**Keywords:** Feature extraction, Ship detection, Speckle noise, Synthetic aperture radar, Tiling.

## OPEN ACCESS

Received: June 24, 2021  
Revised: August 8, 2021  
Accepted: October 14, 2021

**Corresponding Author:**  
Ganesan Kaliyaperumal  
[kganesan@vit.ac.in](mailto:kganesan@vit.ac.in)

 **Copyright:** The Author(s).  
This is an open access article distributed under the terms of the [Creative Commons Attribution License \(CC BY 4.0\)](https://creativecommons.org/licenses/by/4.0/), which permits unrestricted distribution provided the original author and source are cited.

**Publisher:**  
[Chaoyang University of Technology](https://www.cusat.ac.in/)  
ISSN: 1727-2394 (Print)  
ISSN: 1727-7841 (Online)

## 1. INTRODUCTION

Ocean regions in satellite images are useful for a wide range of applications such as surface monitoring, ship monitoring, weather analysis, wind condition estimation and information about the ship traffic (Saleh and Rawashdeh, 2007). Both SAR (Synthetic Aperture Radar) and optical images give plenty of information. Resolutions of the SAR images are high and are less influenced by the weather conditions. Due to the transmission and reception of echoes, SAR images are affected by speckle noise. The optical image is capable of providing useful color features and is also free from speckle noise, and hence it is easy to find the vessels (including all types of ships), and ship wakes. Thus, challenges are high in the case of SAR images when compared to optical images. The types of bands used in the SAR sensor are Ka, Ku, K, S, P, L, C, and X (Dingle Robertson et al., 2020). Each band operates at a particular frequency and wavelength band. Among these eight bands, ship wakes are more visible in C, X,

and L – bands (Yadav et al., 2020). Ship wake detection can provide more information about the ships. The dark center line which corresponds to turbulent wake is generated by the ship hull and Kelvin wakes which are ‘V’ shaped to appear as brighter lines (Tian et al., 2019). These two wake structures are created behind the moving targets (vessel or ship) as shown in the sub-figure from Fig. 3. Unfortunately, due to some reason's wakes are not visible in some situations, particularly at certain radar incident angles, weather states, sea surfaces, and so on. And also, there are no wakes formed while the target is in a stationary position. To overcome these challenges and extract the ocean features, we have concentrated particularly on speckle-noise reduction, ship detection, and wake detection on SAR images. Several studies related to speckle reduction in the SAR images have been carried out in the recent past.

A standard linear filter is applied to reduce the multiplicative speckle noise present in SAR images (Sumantyo and Amini, 2008). Ahmed et al. (2010) have used the patch ordering (shearlet domain) and obtained a better speckle reduction ratio as well as preserved the edge information in the land regions of SAR images and also Wang et al. (2013) have discussed image denoising using unscented Kalman filtering. Li et al. (2009) have got rid of fake objects using the global thresholding method, and also, they have identified the object using the local heterogeneity index in SAR images (Li et al., 2009). Iervolino et al. (2015) have presented a paper wherein they perform the ship detection using Sentinel-1 SAR image by a method known as the Generalized Likelihood Ratio Test (GLRT). Here the land pixels were masked by a technique known as Shuttle Radar Topography Mission (STRM). Jiaqiu et al. (2011) have developed an algorithm that used signal to clutter ratio (SCR) enhancement and Normalized Hough Transform (NHT). In this method, the ship wakes were detected on every divided sub-image.

Sentinel-1 SAR data is despeckled using an evolution of wiener filter, modified using Markov random fields which reduces the complexity of time on the stack of image and also achieves good preservation indexes (Kanoun et al., 2018). Faint Ship wakes are detected in the polarimetric synthetic aperture radar (PolSAR) images using polarization decomposition theory which gives the surface scattering randomness (SSR) parameter that enhances the contrast between sea and wake (Xu et al., 2018). Tings and Velotto (2018) conclude ship wakes are easily identified in the X-band rather than in the C-band.

Tian et al. (2019) have proposed multi-feature recombination and area-based morphological analysis to detect the ship wakes from the TerraSAR-X satellite. This method computes the information about the pixel spatial distance to contour the wake region. Chaturvedi (2019) have introduced the two steps to find the ocean features. First step is to identify the target using Automatic Identification System (AIS) signals by the dead-reckoning (DR) position. Second step is to estimate the speed, position and size of the ship from the SAR images.

Nie et al. (2020) have detected the ships and discriminated the targets using multi-direction high-frequency wavelet coefficients. This method was validated using optical imagery captured using Unmanned Airborne vehicles (UAV). Joseph et al. (2020) have proposed a novel ship detection method using a deep neural network method on the optical satellite image which identifies the ship faster and based on the concept of a convolutional neural network (CNN). Automatic detection algorithm (ADA) has been proposed to extract and analysis the wake texture features. Here, Radon transform is supported to evaluated the L + S decomposition (low rank + sparse) for noise reduction and pixel variation detection (Jose et al., 2021). From the previous study, ship detection in the SAR images are required more time to process and extract the features and false to find the target due to the speckle noise, it impacts the overall performance. In this article, the three essential aspects of the SAR images are focused on, namely speckle, ship detection, and wake feature extraction for velocity estimation. The contributions are framed as follows.

- To improve the feature information and rapid ship detection, standard preprocessing techniques are applied on the proposed tiling with region-based morphological operation on the SAR sensor data.
- The angle and wavelength of ship wake are detected for the estimation of ship velocity using the line-based transform (Radon and Hough transform).
- The processing time and accuracy of the proposed method for ship detection are compared with the previous method.

Section 2 deals with the satellite images used in our experimentation. The tile-based iteration method is discussed in Section 3. Section 4 explains the suitable pre-processing techniques on the SAR sensor data. Section 5 is devoted to tiling with region-based morphological operations involved in ship detection. Section 6 describes the line detection method that can be used for wake detection and discussed the experimental results. Finally, the conclusion is discussed in Section 7.

## 2. EXPERIMENTAL SAR SENSOR DATA

### 2.1 ALOS-2 (PALSAR-2)

The Japan aerospace exploration agency (JAXA) has developed a DAICHI-2 (ALOS-2) satellite which is equipped with Panchromatic L-band Synthetic Aperture Radar (PALSAR-2) with the active microwave L-band radar, PALSAR-2 can monitor the global region such as land deformation, forest and secure navigation of ships. Resolution and a swath of ALOS-2 have enhanced the performance when compared to PALSAR-1 / ALOS-1 (Shimada, 2013). ALOS-2 can provide sufficient information during day and night, in all weather conditions. In this paper, the PALSAR-2 satellite image is used which has taken the image from the region of Denmark on 5th

March 2015. The Strip map has a 10 m resolution with a dual-polarization of HH + HV. The processing level of the product format is level 1.5 (L 1.5) GeoTIFF.

### 3. TILE-BASED ITERATION TECHNIQUE

SAR image processing requires more time to process the ocean features. we have introduced the tiling to reduce the processing time. According to the image size and resolution, one has to fix the tile region such as 4 regions ( $2 \times 2$ ), 9 regions ( $3 \times 3$ ), 16 regions ( $4 \times 4$ ). In this paper, we have used the nine regions i.e. ( $3 \times 3$ ) tiling process on the PALSAR image. The original SAR image is broken into nine regions with the help of the row and column separation method. To reduce the processing time, we have applied  $9 \times 9$  regions tiling to the original image and then perform further analysis, which includes enhancement, speckle filtering, ship detection. The time taken for processing the original image without tiling was 20 minutes.

The processing time is reduced for the SAR images by introducing the tiling technique. In our model, the SAR images are processed into different tiling sizes such as 4-tile, 9-tile, and 16-tile. Due to the tiling process, The computational time is reduced from 20 minutes to 6 minutes (4-tile), 2.5 minutes (9-tile), and 2 minutes (16-tile) respectively. Image information remains the same while using the replicate pixels padding method on each tile size. The pixel range in the image is  $1978 \times 2536$ , where M is the column pixels ( $2536$  divided by  $3$ ), and N is the total row value ( $1978$  divided by  $3$ ). The column tiling blocks are  $1$  to  $M+1$ ,  $M+1$  to  $2M+1$ , and  $2M+1$  to  $2536$ . Likewise,  $1$  to  $N+1$ ,  $N+1$  to  $2N+1$ , and  $2N+1$  to  $1978$  are the row tiling for ( $3 \times 3$ ) 9 regions, as shown in Fig. 1. Each tiled region is processed separately by a standard speckle reduction filter with enhancement (pre-processing) and followed by region-based morphological operation for ship detection. This process is continued until the final iteration (number of tiling regions). The ship detection results are cross-verify using the Sentinel Application Platform (SNAP) tool

(reference). Here, the SNAP tool results are considered as ground truth data.

### 4. PRE-PROCESSING ON THE SAR SENSOR DATA

#### 4.1 Standard Enhancement Approaches and Speckle Noise Filter

The SAR images are processed without any statistical information from metadata lead to limits the image details for further processing. It is necessary to enhance the contrast level to achieve more about those images. There are standard approaches that give better contrast enhancement. In the grey level intensity approach, image pixels values will fill the entire intensity range  $[0, 255]$  and increase the contrast of the image. In bi-histogram equalization Rui and Isa (2016), the distribution of grey levels is achieved for both dark and bright pixels. This method can lead to better details in images that are over or under-exposed.

The adaptive Histogram Equalization (AHE) method differs from the conventional histogram equalization method concerning the adaptiveness of the way that computes several histograms, each corresponding to a distinct section of the image and uses them to redistribute the brightness value of the image. AHE leads to noise amplification in near-constant regions. Contrast Limited AHE (CLAHE) is a variant of the adaptive histogram equalization method in which the contrast amplification is limited, and hence by reduces the problem of noise amplification. CLAHE limits the noise amplification by clipping the histogram at a predefined value before calculating the CDF. It is beneficial if we do not avoid the part of the histogram that exceeds the clip limit but redistributes it equally among all histogram bins and weighted intensity hue saturation for image enhancement (Ma et al., 2017; Schmitt, 2016). Another approach for enhancement is by schmittlets. The definition of the schmittlets is based on the hyperbolic tangent function family employed for the normalization of intensity values

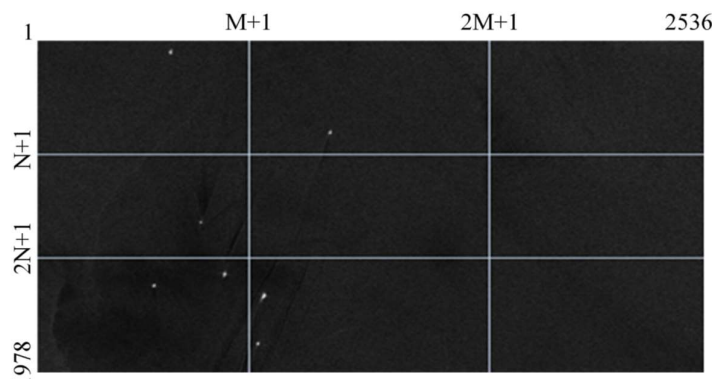


Fig. 1. PALSAR-2/ALOS-2 (L 1.5 GeoTIFF, denmark region, 5<sup>th</sup> March 2015, strip map 10m resolution (HH +HV), 711 MB) with  $3 \times 3$  region tiling technique

of the images. Schmittlets that are exclusively composed out of hyperbolic secant square functions try to increase the solidity of the analysis. After applying schmittlets the image enhancement on stable structures, i.e., deterministic targets achieve better results, but distributed targets are perfectly smoothed. Successive Mean Quantization (SMQT) is mainly preferred for dark regions. As SAR images have some dark regions, one can use this approach explained in Nilsson et al. (2005). In SMQT<sub>L</sub>, L is the number of bits used for describing the level of the transformed image. Where,  $I(x)$  refers to the original image and  $T(x)$  refers to the transformed image from the SMQT process.

$$SMQT_L : I(x) \rightarrow T(x) \tag{1}$$

SMQT<sub>1</sub> means we have a one-bit representation of the image, SMQT<sub>2</sub> means we have a two-bit representation of the image. Likewise, SMQT<sub>8</sub> means we have an 8-bit representation of the image. The steps involved in image transformation are as follows:

**Start**

**Intialize**  $I(x)$  = orignal image

Step1: Calculate the mean (M) of the original image  $I(x)$ .

Step2: Compare the mean value with the pixel value. If the pixel value is smaller than the mean value then replace it with a value of 0. Otherwise, we set a value of 1.

Step3: Again, we calculate the mean of zero-bit pixels values and one-bit pixel values.

Step4: This process is repeated till level 8 and we finally convert the 8-bit binary values into a decimal value.

Step5: In the end, we replace the original pixel value  $I(x)$  with a decimal value of the transformed image  $T(x)$ .

**Stop**

Linear and non-linear filters can be used to reduce the speckle noise, and also one can preserve the edge information present in PALSAR-2/ALOS-2 images. Under the window's pixels calculation, the filters are replacing the center pixel with the calculated value. The standard filters are applied for the important feature information such as median, hybrid median filter, lee, enhanced lee filter, Kuan filter, frost Filter, gamma MAP filter, and Kuwahara filter (Bartyzel, 2016). In this Section, the despeckled image quality is analyzed using EPI and SSIM. The brief discussion about the mathematical concepts related to linear and non-linear filters.

**4.2 EPI and SSIM**

Edge preservation is an essential factor for the evaluation of despeckled images and filters. Edge preservation metrics can be used as the performance index of edge quality. EPI value lies between 0 and 1. If the value is nearly equal to one, the edge information of the image is preserved after filtering (Chumning et al., 2002).

The edge preservation index is evaluated using Equation (2). where  $k$  is the speckled image,  $\hat{k}$  is the despeckled Image,  $\bar{\hat{k}}$  is the mean values of  $\hat{k}$  and  $\bar{k}$  is the mean values of  $k$ .

$$EPI = \frac{\sum(k - \bar{k}, \hat{k} - \bar{\hat{k}})}{\sqrt{\sum(k - \bar{k}, k - \bar{k}) \sum(\hat{k} - \bar{\hat{k}}, \hat{k} - \bar{\hat{k}})}} \tag{2}$$

SSIM is one of the perceptual quantifying metrics which gives the image quality degradation information caused by pre-processing. It measures the perceptual difference between the two similar images. One image is considered as a reference image or original image and another one is a processed image (Guo et al., 2016).

**5. TILING WITH A REGION-BASED MORPHOLOGICAL OPERATION FOR SHIP DETECTION**

Among the enhancement and speckle reduction techniques, we have chosen the grey level to adjust the image intensity value method for enhancement, Lee filter and hybrid median filter for despeckling the PALSAR-2/ALOS-2 ocean region SAR image. After pre-processing, we have applied thresholding (Jin and Wang, 2000; Arshad et al., 2014) and region-based morphological operations to the pre-processed image. The numbers of ships present in the given region of the SAR image are obtained by using thresholding and morphological operations. These objects are specified as white spots, and the remaining water regions are represented as dark spots. The layout of the work done is briefly described in Fig. 2.

Mostly, the combination of erosion and dilation along with the suitable threshold value gives proper perception for ship detection. Erosion is the concept of removal of discontinuous shapes and lines by structural elements. Then, dilation is the process of adding some pixels. Connected-component labeling is usually performed after thresholding. It is an algorithmic application of graph theory, wherein mathematical structures are used to model the pairwise relationships between objects. From the Connected – component labeling, we can measure a set of properties for each connected region (i.e., ships). The actual number of pixels in the connected region is called an area, and the center of mass of the connected region is called a centroid. After finding the centroid coordinates, we have applied the 2D – Euclidean distance transforms to calculate the distance between ships using Equation (3). Let  $(x_1, y_1)$  is the centroid of the Vessel one and  $(x_2, y_2)$  is the centroid of vessel two. Then

$$Distance = \sqrt{(x_2 - x_1)^2 + (y_2 - y_1)^2} \tag{3}$$

Distance between chosen vessels = Distance \* Resolution Range of satellite (10 m).

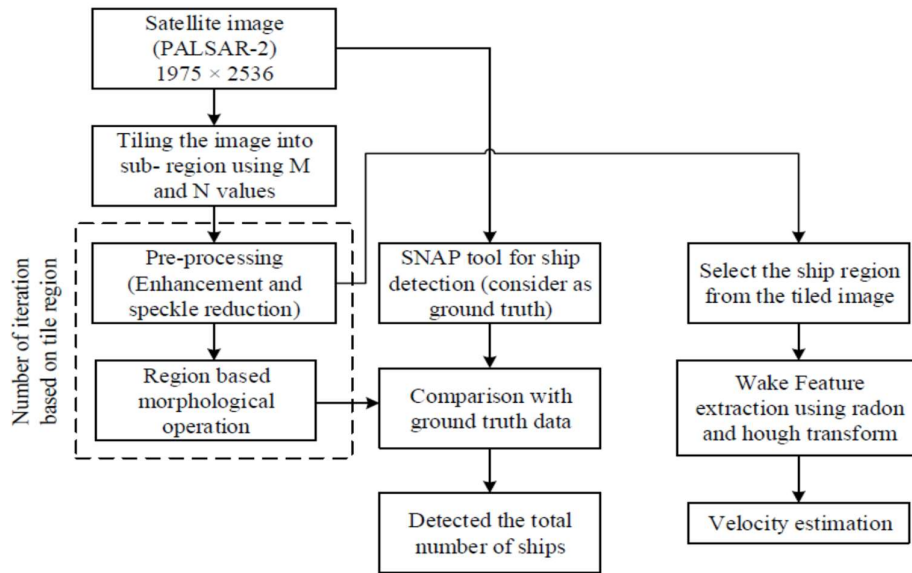


Fig. 2. The block diagram for workflow methodology to process the PALSAR-2 image

5.1 Wake Detection Method

Radon and Hough transform are wake feature extraction or line detection methods. They are manipulated the pixels that present behind the ship using the concept of line identification method to detect the wake lines. Ship with suitable wakes using the sub-image is separated from the statistically processed SAR image, as shown in Fig. 3.

Both Radon and Hough transform is adopted a similar idea to transform the image and found out with lines into line parameters (Van Ginkel et al., 2004). Here,  $\theta$  is the angle and  $\rho$  is the shortest distance to the origin. Parameter  $(\rho, \theta)$  of Radon transform (Jose et al., 2021) is an integration of line through the image  $f(p, q)$  with the value of  $\rho$  and  $\theta$  which corresponds to the line in the image and Dirac delta function ( $\delta$ ) as shown in Equation (4).

$$Y(\rho, \theta) = \iint_{-\infty}^{\infty} f(p, q) \delta(\rho - p \cos \theta - q \sin \theta) dpdq \quad (4)$$

Then the Line expression can be written as in Equation (5) below:

$$\rho = p \cos \theta + q \sin \theta \quad (5)$$

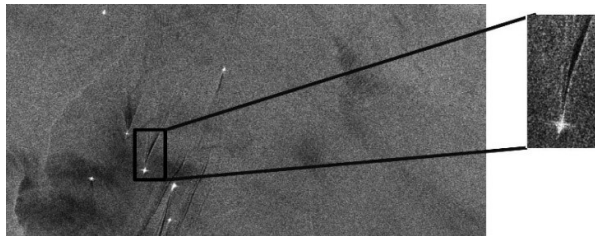


Fig. 3. Ship region separation from PALSAR-2 for wake detection (present behind the ship)

In Hough transform Jiaqiu et al. (2011), all possible  $\rho$  and  $\theta$  values are stored in the accumulator space (array) and then using the maximum peak value from this array, one can draw the lines with ship centroid point as indicated in Fig. 4. Both the methods are trying to find the horizontal and vertical lines while scanning the image in all directions. Hough transform takes the radial distance of a point towards the origin in all directions; whereas Radon

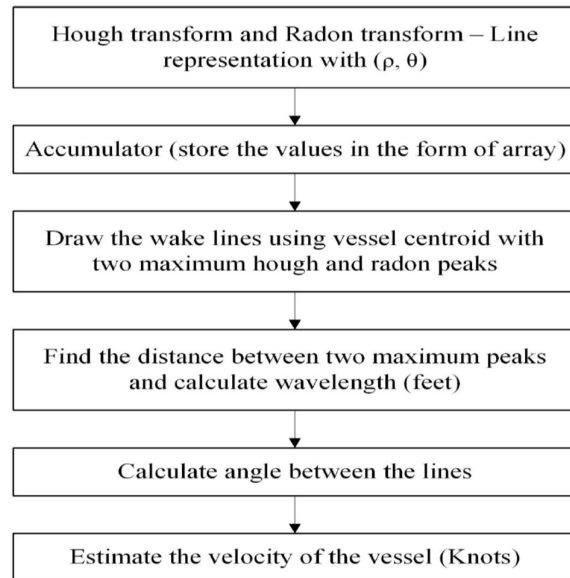


Fig. 4. The flow diagram of Radon and Hough transform method to detect lines from ship wakes

transform takes the radial line perpendicular to the line joining the point to the origin in all directions.

After wake lines detection, we have calculated the angle between the two lines in the given SAR image, which is valuable for estimating the ship velocity using Equation (6).

$$v = \sqrt{\frac{g\lambda}{2\pi \sin \theta}} \quad (6)$$

Here,  $g$  is the acceleration due to gravity,  $\lambda$  is the wavelength which is the distance between two maximum peaks and then, multiplies it with the resolution of the image (Lu et al., 2017; Graziano et al., 2016).  $\theta$  is the angle between the wake lines and  $v$  is the velocity of the ship. Equation (6) is used for finding the velocity of a ship (Zilman et al., 2004).

## 6. RESULTS AND DISCUSSION

The tile-based iteration method performs the subsequent pre-processing on the tiled images that leads to less computational complexity rather than processing the whole image for detecting the ship. In the pre-processing step, we have implemented different enhancement and filtering techniques for detecting the ships. Our implementation

with image tiling that provides lesser processing time for speckle reduction and ship detection. The enhancement results and wave detection of our experiment are discussed below subsections.

### 6.1 Image Enhancement Results

Among the five techniques, adjust the image intensity values method is found to be the best when compared to all other methods. SMQT consumes more time for processing as well as the visual quality of the image gets degraded. For the remaining methods (Histogram equalization, Contrast-limited adaptive histogram equalization, Schmittlets), the processing time is less and degrades the ship information after enhancement. Thus, adjust the image intensity values method is a better pre-processing method on SAR images is shown in Fig. 5. Also, the Contrast Improvement Index (CII) metrics (Subramani et al., 2018) are estimated for different enhancement techniques as presented in Table 1. The image quality (pixel intensity) is improved when compared to the original SAR image using adjust the image intensity values method. From Table 1, adjust the image intensity values method is chosen for further processing.

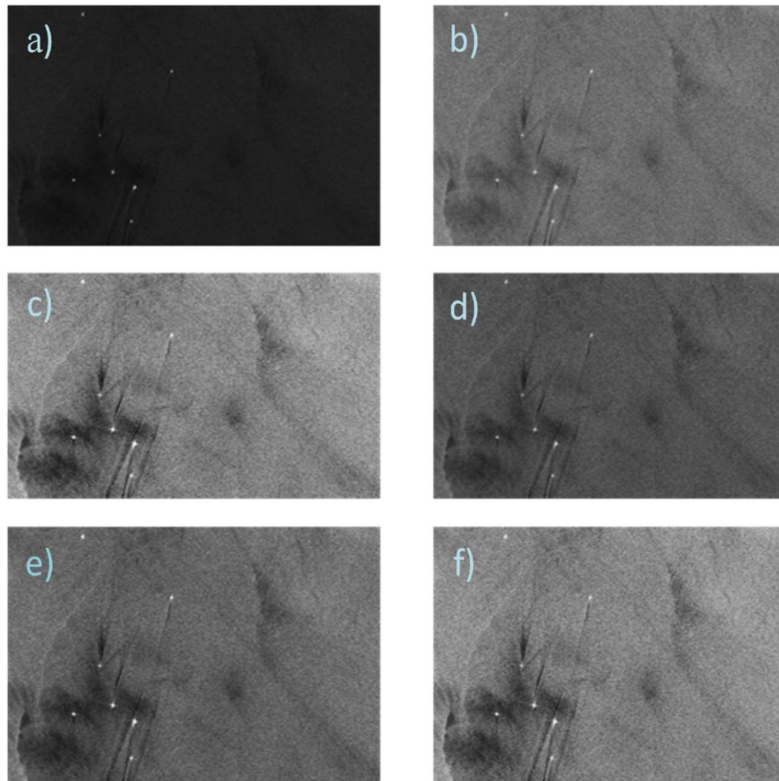


**Fig. 5.** Different enhancement techniques (a) Original SAR image (b) Adjust image intensity values method of enhancement (c) Histogram equalization (d) Contrast limited adaptive equalization (e) Successive mean quantization transform (SMQT) (f) Schmittlets enhancement

**Table 1.** CII analysis for different enhancement techniques

Contrast for the original image	Enhancement Techniques	CII for the preprocessed image
0.521	Adjust image intensity method	0.778
	HE	0.649
	CLAHE method	0.703
	SMQT method	0.757
	Schmittlets method	0.640

**6.2 Comparison Results for Different Speckle Filtering**

According to the window size, SAR images are despeckled and the edges are preserved, as shown in Fig. 6. The comparison based on the metric, namely EPI and SSIM for all speckle filters is shown in Table 2 below. The EPI and SSIM values are observed as follows: Median (0.4641) (0.7889), Hybrid median (0.5399) (0.7915), Lee

(0.5539) (0.7806), Enhanced lee (0.6016) (0.7762), Frost (0.5132) (0.7419), Kuan (0.4689) (0.7265), Kuwahara (0.4563) (0.7715), Gamma MAP (0.4986) (0.7521) for the SAR image. EPI is better in the case of enhanced lee filter, but the time required to process it is high when compared to the lee filter and hybrid median filters. Based on our analysis, we recommend Lee or hybrid median filters for further analysis.

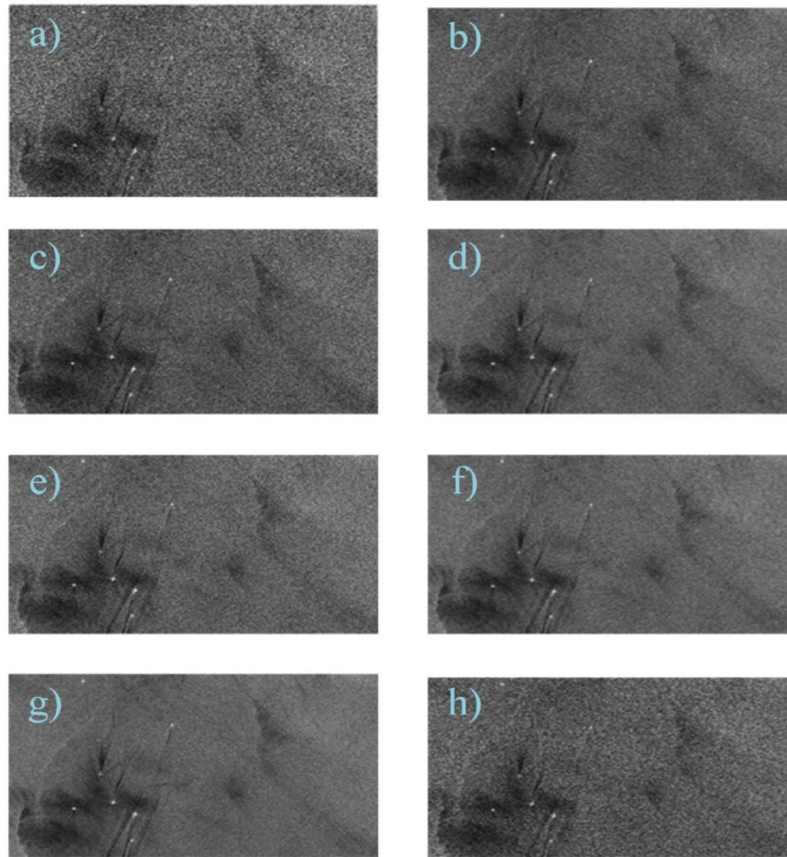


**Fig. 6.** Different speckle-noise filters (a) Image with speckle noise (b) Despeckling using median filter (c) Kuwahara filter (d) Hybrid median (e) Enhanced lee filter (f) Frost filter (g) Kuan filter (h) Gamma MAP filter

**Table 2.** Edge preservation index for different speckle filters of size  $3 \times 3$  kernels

S. No	Filter	EPI	SSIM
1	Median	0.4641	0.7889
2	Hybrid Median Filter	0.5399	0.7915
3	Lee Filter	0.5539	0.7806
4	Enhanced Lee Filter	0.6016	0.7762
5	Kuan Filter	0.4689	0.7265
6	Frost Filter	0.5132	0.7419
7	Kuwahara Filter	0.4563	0.7715
8	Gamma MAP Filter	0.4986	0.7521

6.3 Ship Detection Results

Region-based morphological operations are applied on each tile separately. we have found the ships in the ocean region of a given satellite image (PALSAR-2) is shown in

Fig. 7 and Fig. 8. Ship detection results are compared with the existing results as shown in Table 3. Once the ships are detected, we can find the distance between the ships.

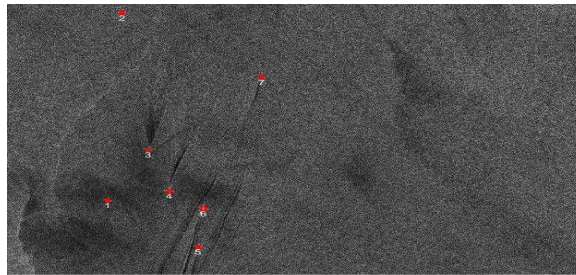


**Fig. 7.** Detection of vessels/ships from PALSAR-2 satellite image (Denmark region)

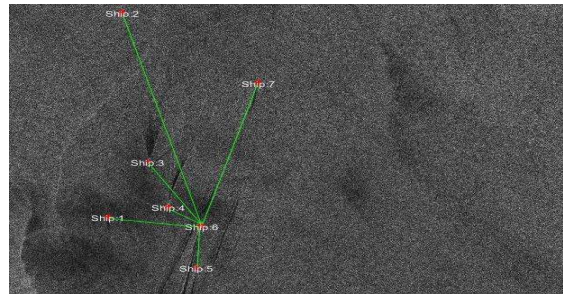


**Fig. 8.** Calculation of the distance between ship 6 and all other ships

**Table 3.** Ship detection results compared with the existing method

Detected methods	Total number of ships	Number of ships detected	Number of real ships detected	
Yang et al. (2013)	364	399	356 (97.8%)	
Proia and Pagé (2009)	364	420	329 (78.3%)	
Corbane et al. (2010)	364	359	317 (88.3%)	
Bi et al. (2012)	364	391	336 (92.3%)	
Tile-based iteration method followed by morphological operation $1978 \times 2536$ (proposed method)	Tile 1	1		
	Tile 2	1		
	Tile 3	0		
	Tile 4	1	7	7
	Tile 5	0		
	Tile 6	0		
	Tile 7	2		

The distance calculated between ship 6 and all other ships in nautical miles is highlighted in Table 4. The processing time for ship detection of the proposed method has compared with standard existing model as shown in Table 5. The improvement is obtained by 1.0 times to 1.5 times.

**Table 4.** Distance between the ship 6 and all other ships in nautical miles

Distance between the ship (nautical mile)		
Ship 6	Ship 1	122.146
	Ship 2	430.743
	Ship 3	140.992
	Ship 4	52.842
	Ship 5	76.859
	Ship 7	287.786

6.4 Wake Detection Results

Both Radon and Hough transform have the property of detecting the lines that are used to estimate the velocity of

the ship from 'V' shaped wake lines behind the ship. The key factors to find the velocity of the ships are satellite image wavelength and peak values present in Radon and Hough transform, and then the velocity is calculated by using [6] the wavelength, acceleration due to gravity at sea level (constant value is 9.806 m/s<sup>2</sup>) and the angle between the two lines (i.e., 'V' shaped wakes) in the image as shown in Fig. 9 and Fig. 10. in terms of knots.

The tile-7 region (ship 4) velocity is estimated using Equation (6) The velocity of ship 4 is 10.993 knots and 11.53 knots using Hough and Radon transform. Since ground truth data are not available to validate the velocity estimation, but the results are compared with two feature extraction methods (Radon and Hough transform). The algorithm has been performed on a personal computer with an Intel(R) Core (TM) i5-4590 CPU @ 3.30GHz, 4 Core, and 8 GB of RAM. We have selected the data product from PALSAR-2/ALOS-2 at level 1.5 (L1.5) in GeoTIFF format with a resolution of 1978 × 2536.

**Table 5.** Comparison of the processing time for ship detection in a satellite image

Processing time in second (s)		
Speckle reduction and wake detection of SAR image size 1978 × 2536 (Proposed method)	Tile with a region-based morphological method	160
Optical image of size 9000 × 9000 (Tian et al., 2019)	SDSSA method	72
Optical image of size 9000 × 9000 (Proia and Pagé, 2009)	Bayesian decision theory	171
Optical image of size 9000 × 9000 (Corbane et al., 2010)	Morphology with wavelet method	254
Optical image of size 9000 × 9000 (Bi et al., 2012)	Neighbourhood similarity-based method	227

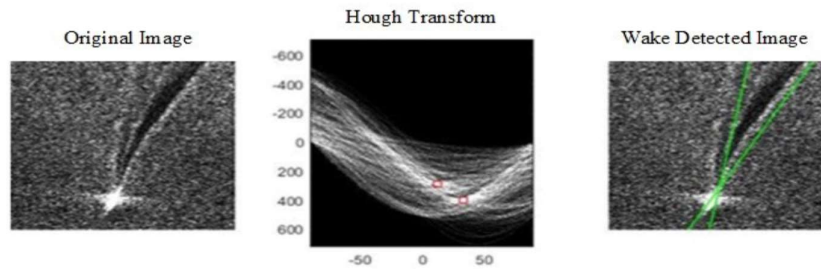


**Fig. 9.** The method of hough transform for wake line detection from the tiled image (wavelength 68.59 feet and velocity 10.993 knots)

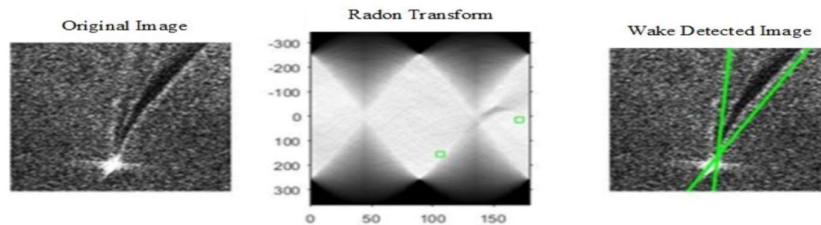


**Fig. 10.** Radon transform method for wake detection from the tiled satellite image (wavelength 75.31 feet, velocity 11.53 knots)

## 7. CONCLUSION

In this work, the proposed model has detected the ship using tile-based iteration method and wakes features extracted for velocity estimation using Radon and Hough transform from the PALSAR-2/ALOS-2 satellite imagery of Synthetic Aperture Radar (SAR) sensor. The design is implemented into three modules such as pre-processing, ship detection, and wake detection for ship velocity estimation. The performance analysis of pre-processing is evaluated using the edge preservation index (EPI) and Structure Similarity Index (SSIM) metrics. Tiling with region-based morphological operations of the ship detection method is suitable to detect the ships from the despeckled images of strip map mode with 10m resolution. Our method provides a lesser processing time of 1.5 times than the standard existing models. Ship velocity is evaluated by the angle and wavelength from the detected wake lines using Radon transform and Hough transform. From the analysis, both transforms of Radon and Hough are noticed that the Radon transform gives precise results than the Hough transform and also achieves the processing time for ocean feature extraction from the satellite imagery.

## ACKNOWLEDGMENT

The authors would like to thank the Director, NPOL for his support and encouragement. We express our gratitude to Vellore Institute of Technology, Vellore for providing us with the infrastructure. The authors are grateful for the satellite data provided by the Japan Aerospace Exploration Agency (JAXA) and the European Space Agency (ESA).

## REFERENCES

- Ahmed, S.M., Eldin, F.A.E., Tarek, A.M. 2010. Speckle noise reduction in SAR images using adaptive morphological filter. In 2010 10th International Conference on Intelligent Systems Design and Applications. 260–265.
- Arshad, N., Moon, K.S., Kim, J.N. 2014. Adaptive real-time ship detection and tracking using morphological operations. *Journal of information and communication convergence engineering*, 12, 168–172.
- Bartyzel, K. 2016. Adaptive kuwahara filter. *Signal, Image and Video Processing*, 10, 663–670.
- Bi, F., Zhu, B., Gao, L., Bian, M. 2012. A visual search inspired computational model for ship detection in optical satellite images. *IEEE Geoscience and Remote Sensing Letters*, 9, 749–753.
- Chaturvedi, S.K. 2019. Study of synthetic aperture radar and automatic identification system for ship target detection. *Journal of Ocean Engineering and Science*, 4, 173–182.
- Chumning, H., Huadong, G., Changlin, W. 2002. Edge preservation evaluation of digital speckle filters. In *IEEE International Geoscience and Remote Sensing Symposium*. 2471–2473.
- Corbane, C., Najman, L., Pecoul, E., Demagistri, L., Petit, M. 2010. A complete processing chain for ship detection using optical satellite imagery. *International Journal of Remote Sensing*, 31, 5837–5854.
- Dingle Robertson, L., Davidson, A.M., McNairn, H., Hosseini, M., Mitchell, S., de Abelleira, D., Verón, S., Le Maire, G., Plannells, M., Valero, S., Ahmadian, N. 2020. C-band synthetic aperture radar (SAR) imagery for the classification of diverse cropping systems. *International Journal of Remote Sensing*, 41, 9628–9649.
- Graziano, M.D., D’Errico, M., Rufino, G. 2016. Ship heading and velocity analysis by wake detection in SAR images. *Acta astronautica*, 128, 72–82.
- Guo, J.H., Yang, F., Tan, H., Wang, J.X., Liu, Z.H. 2016. Image matching using structural similarity and geometric constraint approaches on remote sensing images. *Journal of Applied Remote Sensing*, 10, 045007.
- Iervolino, P., Guida, R., Whittaker, P. 2015. A novel ship-detection technique for Sentinel-1 SAR data. In *2015 IEEE 5th Asia-Pacific Conference on Synthetic Aperture Radar (APSAR)*. 797–801.
- Jiaqiu, A., Xiangyang, Q., Weidong, Y., Yunkai, D., Fan, L., Li, S., Yafei, J. 2011. A novel ship wake CFAR detection algorithm based on SCR enhancement and normalized Hough transform. *IEEE Geoscience and Remote Sensing Letters*, 8, 681–685.
- Jin, Y.Q., Wang, S.Q. 2000. An algorithm for ship wake detection from the synthetic aperture radar images using the Radon transform and morphological image processing. *The Imaging Science Journal*, 48, 159–163.
- Jose, F.J., Rajesh, M., Rajan, V. 2021. Development of wake detection and analysis by using image processing. In *Computer Networks and Inventive Communication Technologies (519–529)*. Springer, Singapore.
- Joseph, S.I.T., Sasikala, J., Juliet, D.S. 2020. Detection of ship from satellite images using deep convolutional neural networks with improved median filter. In *Artificial Intelligence Techniques for Satellite Image Analysis*. 69–82.
- Kanoun, B., Ferraioli, G., Pascazio, V., Schirinzi, G. 2018. Fast algorithm for despeckling sentinel-1 SAR data. In *EUSAR 2018; 12th European Conference on Synthetic Aperture Radar*. 1–5.
- Li, W., He, M., Zhang, S. 2009. A heterogeneity-based ship detection algorithm for SAR imagery. In *2009 2nd International Congress on Image and Signal Processing*. 1–5.
- Lu, Y., Zhuang, X., Sun, Z., Wang, S., Liu, W. 2017. Wavelength estimation method based on radon transform and image texture. *Journal of Shipping and Ocean Engineering*, 7, 186–191.

- Ma, J., Zou, C., Jin, X. 2017. An improved image enhancement algorithm. *Wuhan University Journal of Natural Sciences*, 22, 85–92.
- Nie, T., Han, X., He, B., Li, X., Liu, H., Bi, G. 2020. Ship detection in panchromatic optical remote sensing images based on visual saliency and multi-dimensional feature description. *Remote Sensing*, 12, 152.
- Nilsson, M., Dahl, M., Claesson, I. 2005. The successive mean quantization transform. In *Proceedings. (ICASSP'05)*. IEEE International Conference on Acoustics, Speech, and Signal Processing. iv–429.
- Proia, N., Pagé, V. 2009. Characterization of a Bayesian ship detection method in optical satellite images. *IEEE Geoscience and Remote Sensing Letters*, 7, 226–230.
- Rui, T.J., Isa, N.A.M. 2016. Intensity exposure-based bi-histogram equalization for image enhancement. *Turkish Journal of Electrical Engineering and Computer Science*, 24, 3564–3585.
- Saleh, B., Rawashdeh, S. 2007. Study of urban expansion in Jordanian cities using GIS and remote sensing. *International Journal of Applied Science and Engineering*, 5, 41–52.
- Schmitt, A. 2016. Multiscale and multidirectional multilooking for SAR image enhancement. *IEEE Transactions on Geoscience and Remote Sensing*, 54, 5117–5134.
- Shimada, M. 2013. ALOS-2 science program. In *2013 IEEE International Geoscience and Remote Sensing Symposium-IGARSS*. 2400–2403.
- Subramani, B., Veluchamy, M. 2018. MRI brain image enhancement using brightness preserving adaptive fuzzy histogram equalization. *International Journal of Imaging Systems and Technology*, 28, 217–222.
- Sumantyo, J.T.S., Amini, J. 2008. A model for removal of speckle noise in SAR images (ALOS PALSAR). *Canadian Journal of Remote Sensing*, 34, 503–515.
- Tian, M., Yang, Z., Mao, Z., Liao, G. 2019. Ship wake region detection by using multi-feature recombination and area-based morphological analysis in ATI-SAR systems. *The Journal of Engineering*, 7397–7402.
- Tings, B., Velotto, D. 2018. Comparison of ship wake detectability on C-band and X-band SAR. *International Journal of Remote Sensing*, 39, 4451–4468.
- Van Ginkel, M., Hendriks, C.L., Van Vliet, L.J. 2004. A short introduction to the Radon and Hough transforms and how they relate to each other. Delft University of Technology.
- Wang, R., Li, S., Kuruoglu, E.E. 2013. A novel algorithm for image denoising based on unscented Kalman filtering. *International Journal of Information and Communication Technology*, 5, 343–353.
- Xu, Z., Tang, B., Cheng, S. 2018. Faint ship wake detection in PolSAR images. *IEEE Geoscience and Remote Sensing Letters*, 15, 1055–1059.
- Yadav, V.P., Prasad, R., Bala, R., Srivastava, P.K. 2020. Synergy of vegetation and soil microwave scattering model for leaf area index retrieval using C-band sentinel-1A satellite data. *IEEE Geoscience and Remote Sensing Letters*.
- Yang, G., Li, B., Ji, S., Gao, F., Xu, Q. 2013. Ship detection from optical satellite images based on sea surface analysis. *IEEE Geoscience and Remote Sensing Letters*, 11, 641–645.
- Zilman, G., Zapolski, A., Marom, M. 2004. The speed and beam of a ship from its wake's SAR images. *IEEE Transactions on Geoscience and Remote Sensing*, 42, 2335–2343.